

## Article

# Surface Modification of WE43 Magnesium Alloys with Dopamine Hydrochloride Modified GelMA Coatings

Yang Ji <sup>1,†</sup>, Mengdie Hou <sup>2,†</sup>, Jin Zhang <sup>2</sup>, Tianlin Wang <sup>2</sup> , Can Cao <sup>1,\*</sup>, Huazhe Yang <sup>2,\*</sup>  and Xiaodong Zhang <sup>1,\*</sup>

<sup>1</sup> Department of Stomatology, General Hospital of Northern Theater Command, Shenyang 110016, China; yangji2080@163.com

<sup>2</sup> School of Intelligent Medicine, China Medical University, Shenyang 110122, China; hougengdie1@163.com (M.H.); zhangjin01152022@163.com (J.Z.); tlwang@cmu.edu.cn (T.W.)

\* Correspondence: caocanevan1988@outlook.com (C.C.); hzyang@cmu.edu.cn (H.Y.); zyxdzhang@163.com (X.Z.)

† These authors contributed equally to this work.

**Abstract:** As biodegradable medical implants, magnesium alloys have attracted great concerns due to their desirable biological and mechanical performances. Nevertheless, the overfast degradation rate of magnesium alloys makes it difficult to make full use of their potential in medical sciences. Therefore, it is a hot issue to control the degradation rate and functionalize the magnesium alloys via surface modifications. Herein, methacrylate gelatin (GelMA) hydrogel was adopted as coatings on the surface of WE43 magnesium alloys to control the degradation behaviors of magnesium alloys. Inspired by mussels, dopamine (DOPA) hydrochloride was adopted to modify GelMA to further functionalize the coatings. The compositions, swelling properties, degradation behaviors, and morphologies of samples were characterized by UV-Vis spectrophotometer, nuclear magnetic resonance (NMR), Fourier transform infrared spectroscopy (FTIR), scanning electron microscope (SEM), and immersion test. It was shown that GelMA-DOPA composites could be obtained and the swelling and degradation behaviors of magnesium alloys could be controlled by adjusting the compositions of GelMA and DOPA. Furthermore, the GelMA-DOPA hydrogel coatings can be tightly bonded to the Mg alloys.

**Keywords:** composite coatings; gelma hydrogel; magnesium alloys; surface modifications



**Citation:** Ji, Y.; Hou, M.; Zhang, J.; Wang, T.; Cao, C.; Yang, H.; Zhang, X. Surface Modification of WE43 Magnesium Alloys with Dopamine Hydrochloride Modified GelMA Coatings. *Coatings* **2022**, *12*, 1074. <https://doi.org/10.3390/coatings12081074>

Academic Editor: Philipp Vladimirovich Kiryukhantsev-Korneev

Received: 21 June 2022

Accepted: 28 July 2022

Published: 29 July 2022

**Publisher's Note:** MDPI stays neutral with regard to jurisdictional claims in published maps and institutional affiliations.



**Copyright:** © 2022 by the authors. Licensee MDPI, Basel, Switzerland. This article is an open access article distributed under the terms and conditions of the Creative Commons Attribution (CC BY) license (<https://creativecommons.org/licenses/by/4.0/>).

## 1. Introduction

Nowadays, magnesium (Mg) alloys have attracted considerable attention and become one of the most promising candidates as bone implants due to their excellent biocompatibility, biodegradability, mechanical compatibility, osteogenesis inductivity, antibacterial ability, etc. [1–5]. The clinical development of Mg alloys, however, is hindered owing to their overfast degradation rate [6]. As a result, Mg alloys cannot stably provide mechanical support and perform the biological functions to repair large bone defects (e.g., large jaw defects) [7]. Furthermore, a large amount of Mg<sup>2+</sup> ions and excess hydrogen gas released during the corrosion of Mg alloys could result in biological problems such as cytotoxicity and delay of bone formation [8,9]. As a solution, surface modification is considered a feasible way to control the degradation rate and improve the corrosion resistance of Mg alloys [10,11].

To date, various surface modification techniques, i.e., micro-arc oxidation (MAO) [12,13], electrochemical deposition [14,15], chemical conversion [16,17], dip-coating [18], etc., have been devised and applied to treat bare Mg alloys to control the degradation rate and functionalize the surface of Mg alloys. However, there is a lack of an “ideal” one-step technique to achieve the goals of degradation control and functionalization [10]. For instance, the MAO technique has been widely applied and considered to be one of the most effective ways to reduce the corrosion rate of Mg alloys [19,20], because the MAO coatings

fabricated on the surface of Mg alloys have strong adhesion [21] and wear resistance [22]. However, as a ceramic layer, MAO coatings are inert and are not conducive to cell adhesion and growth. In addition, micro-pores and micro-cracks are unavoidable in the MAO coatings, which is harmful for the protection of Mg alloys [23]. Accordingly, a post-treatment of MAO is necessary to enhance the biocompatibility as well as to seal the pores/cracks of MAO coatings [24,25].

Fabricating composite coatings based on the MAO technique is one of the most attractive post-treatment strategies [26,27]. Especially, coatings with various functions (such as bioactivities) are favorable to endow Mg alloys with tunable properties [28]. Recently, as an extracellular matrix (ECM) mimicking material, gelatin methacrylate (GelMA) hydrogel is remarkable [29]. GelMA hydrogel [30,31] is a kind of photocrosslinked hydrogel, which can be formed by free radical polymerization under the condition of photoinitiation. It has aroused considerable interest due to its tunable physicochemical properties, excellent compatibilities, and bioactivities. In a previous study, we deposited GelMA hydrogel coatings with varying thicknesses on the surface of MAO-coated Mg alloys via a dip-coating method [32], and both the corrosion resistance and the compatibility improved compared with those without the GelMA coatings. However, as biodegradable implants, the debris of MAO coating formed during the degradation process of Mg alloys may have potential biosafety issues since the MAO coating is nondegradable. In addition, the adhesion between GelMA hydrogel coating and MAO coating is weak, which may cause the GelMA hydrogel coating to peel off. Also, two steps, i.e., MAO process and dip-coating process, were adopted to prepare the hydrogel/MAO composite coatings, which increases the complexity and difficulties of the experiment. As an alternative, it is favorable to deposit GelMA hydrogel coatings directly on the surface of Mg alloys from the perspective of biocompatibility of implants as well as the operability of the experiment. However, the adhesion between GelMA hydrogel and Mg alloys is also weak due to the great difference between the mentioned two types of materials [33].

Herein, we tried to further optimize the GelMA hydrogel as coatings for Mg alloys. The mussel-inspired hydrogel was devised and proposed to modify GelMA hydrogel with dopamine (DOPA) hydrochloride, and the GelMA-DOPA hydrogel coatings were deposited on the surface of Mg alloys directly via a dip-coating technique. The GelMA-DOPA has catechol groups that can form coordination bonds with metal ions, which may provide a promising way to enhance the bonding ability between hydrogels and Mg alloys and is expected to further functionalize the Mg alloys. This strategy can provide novel insights into the surface modifications and applications of Mg alloys.

## 2. Materials and Methods

### 2.1. Materials

Mg alloys (WE43, Mg-4% Y-3.3% RE (Nd, Gd)-0.5% Zr) were purchased from Wuxi Taicheng Metal Material Products Co. Ltd. (Shenzhen, China), and these materials were cut into pellets with  $\Phi 10$  mm, followed by polishing with abrasive papers and washing with ethanol (99.7%) ultrasonically. Gelatin and photoinitiator (Irgacure 2959, 98%) were purchased from Shanghai Yuanye Biotechnology Co. (Shanghai, China), Methacrylic Anhydride (MA, 94%) was purchased from Sigma-Aldrich (St. Louis, MO, USA), Succinic anhydride (98%), triethylamine (99%), dimethyl sulfoxide (99%), 2-Morpholinoethanesulphonic acid (MES) buffer (pH = 5.5), dopamine hydrochloride (98%), N-Hydroxysuccinimide (NHS, 98%) and N(3-dimethylaminopropyl)-n1-Ethylcarbodiimide hydrochloride (EDC, 98%) were purchased from Macklin Inc., China (Shanghai, China). Phosphate buffered solution (PBS) was purchased from Hyclone (Logan, UT, USA), and Collagenase Type II (Collagenase) was purchased from Beijing Solaibao Technology Co., Ltd. (Beijing, China). Dialysis tube (10K MWCO, 22 mm) was purchased from Thermo Fisher Scientific (Rockford, IL, USA).

## 2.2. Methods

The schematic flowchart for the preparation of the GelMA-DOPA coated Mg alloy composites and the relative mechanisms to synthesize GelMA and GelMA-DOPA hydrogels is shown in Figure 1.

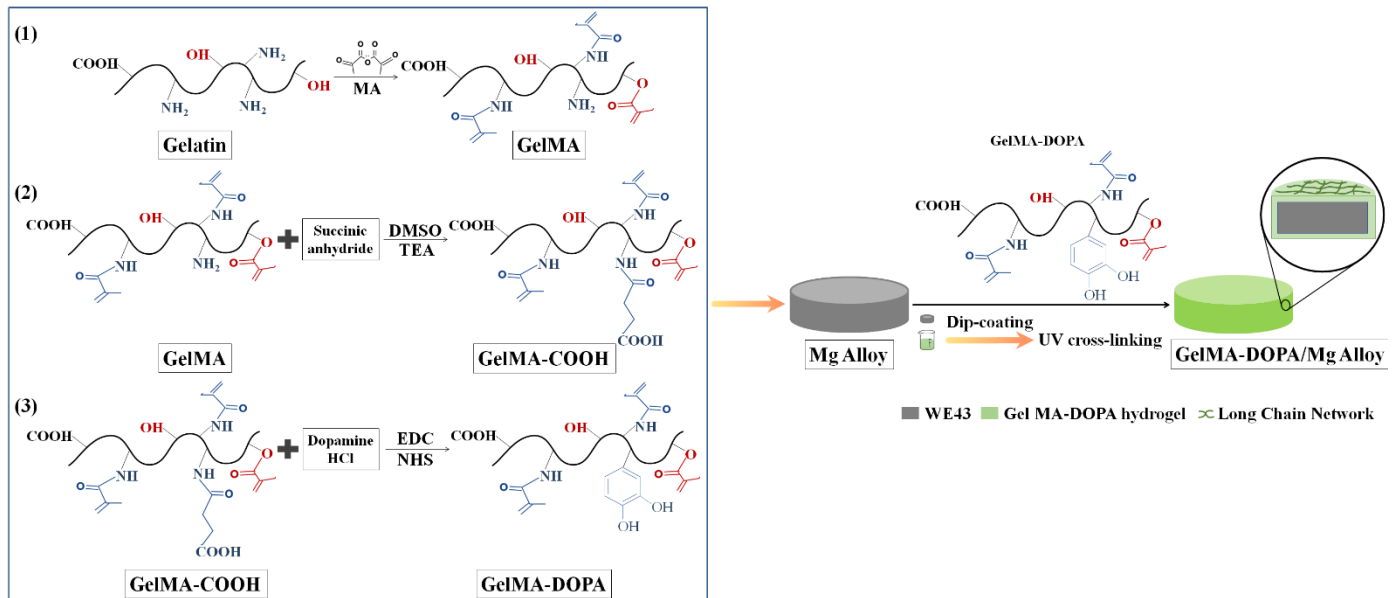


**Figure 1.** Schematic flow chart of the process and mechanisms of preparing GelMA-DOPA hydrogel/Mg alloy composites.

### 2.2.1. Synthesis of GelMA Prepolymer

The synthesis method of GelMA prepolymer was described previously [34]. Briefly, 10 g of gelatin was dissolved into 200 mL of PBS. Afterwards, 16 mL of MA was added dropwise to the gelatin solution using a micro syringe pump at a rate of 0.2 mL/min, followed by reacting for 2 h by stirring at 50 °C. Then the mixed solution was diluted by 200 mL of PBS and dialyzed in deionized water for 10 days. Subsequently, 400 mL of deionized water was added into the dialytic solution and stirred for 15 min. Finally, the solution was packed in centrifuge tubes, and lyophilized for 4 days to obtain GelMA prepolymer.

### 2.2.2. Synthesis of GelMA-COOH Prepolymer

2 g of the GelMA prepolymer was dissolved in 20 mL of PBS, stirring at 50 °C to obtain a homogeneous solution. A total of 1 mL of triethylamine, 1 g of succinic anhydride and 20 mL of dimethyl sulfoxide were added into the solution, and then stirred for 12 h at 50 °C, followed by diluting with 100 mL of PBS solution. The excess triethylamine was neutralized with 0.1 M hydrochloric acid solution. Finally, the solution was dialyzed with deionized water for 1 week at room temperature using a dialysis tube in order to remove impurities in the solution. The dialyzed solution was placed in a centrifuge tube and frozen in a refrigerator at −80 °C for two days, and then freeze-dried for 4 days to obtain GelMA-COOH prepolymer.

### 2.2.3. Synthesis of GelMA-DOPA Prepolymer

1 g of the as-prepared GelMA-COOH was dissolved in 10 mL of MES buffer, and it was degassed with nitrogen for 15 min. Afterwards, 0.2 g of EDC, 0.3 g of NHS and 0.2 g of dopamine hydrochloride were added to the solution, and then stirred at a temperature of 25 °C for 12 h under nitrogen. Then, it was dialyzed for 4 days in 0.01 M hydrochloric acid solution using a dialysis tube, followed by neutralizing to pH = 7 with 0.01 M of sodium hydroxide. Finally, the solution was packed into centrifuge tubes and frozen in a

refrigerator at  $-80\text{ }^{\circ}\text{C}$  for two days, after which it was freeze-dried for four days to obtain GelMA-DOPA prepolymers.

#### 2.2.4. Preparation of GelMA-DOPA/Mg Composites

The GelMA-DOPA (Experimental group) and GelMA (Control group) prepolymers were respectively dissolved in PBS at room temperature with concentrations of 5% ( $w/v$ ), 10% ( $w/v$ ), 15% ( $w/v$ ) and 20% ( $w/v$ ), and then 1% ( $w/v$ ) of photoinitiator was dissolved into the mixed solution through ultrasonic agitation. Mg alloy pellets were dipped into the GelMA and GelMA-DOPA solutions for 1 min. Afterwards, the Mg alloys were withdrawn at a constant speed of 1 cm/min. After cross-linking the prepolymer layer in UV (365 nm, 10  $\text{mw}/\text{cm}^2$ ) for 5 min, GelMA-DOPA and GelMA hydrogel coating formed on the surface of Mg alloys. The above dipping-coating process was repeated 3 times.

#### 2.2.5. Characterizations

Fourier transform infrared spectroscopy (FTIR-850, Tianjin Gangdong Technology Co., Ltd., Tianjin, China), UV-Vis spectrophotometer (T6 New Centroy, Beijing Puxi General Instrument Co., Ltd., Beijing, China), and nuclear magnetic resonance (NMR, Mercury-Vx300-NMR, Varian, Palo Alto, CA, USA) were adopted to analyze the compositions, contents and chemical groups of the samples. A scanning electron microscope (SEM, JSM-7001F, JEOL, Tokyo, Japan) was adopted to observe the morphologies of the samples.

The swelling ratios of the samples were characterized as follows: The GelMA-DOPA and GelMA prepolymers were dissolved in PBS containing 1% ( $w/v$ ) Irgacure 2959 to prepare solutions with concentrations of 5% ( $w/v$ ), 10% ( $w/v$ ), 15% ( $w/v$ ) and 20% ( $w/v$ ), respectively. The solutions were added dropwise to cylindrical moulds ( $\Phi 6$  mm, height: 3 mm) and irradiated under UV for 7 min to obtain cylindrical hydrogel pellets (dry weight  $W_d$ ). Then, the hydrogel pellets were immersed in PBS solution, swelling for different time intervals (1 h, 2 h, 4 h, 8 h, 12 h, 24 h, and 48 h, respectively), and were weighed ( $W_s$ ) after the excess PBS being dried with filter paper. The swelling rates of both GelMA-DOPA and GelMA hydrogels can be calculated according to the following equation.

$$\text{Swelling ratio} = (W_s - W_d)/W_s \quad (1)$$

The weights of pellets were calculated at swelling equilibrium ( $W_e$ ) in the swelling test, and then the samples were immersed in 2  $\mu\text{g}/\text{mL}$  of type II collagenase PBS at  $37\text{ }^{\circ}\text{C}$ . The mass of the hydrogel was recorded at a fixed time each day as  $W_t$  and the degradation rate of the hydrogels with different concentrations was calculated according to the following equation:

$$\text{Degradation rate} = (W_e - W_t)/W_e \quad (2)$$

### 3. Results

#### 3.1. Chemical groups of samples

Figure 2A shows the IR spectra of GelMA, GelMA-COOH and GelMA-DOPA. A typical IR spectrum of GelMA can be identified: the peaks around  $3300\text{ cm}^{-1}$  represent the stretching vibration of  $-\text{OH}$  groups and  $\text{N}-\text{H}$  groups, while peaks around  $1500\text{ cm}^{-1}$  are due to the bending vibration of  $\text{N}-\text{H}$  groups. The peaks around  $2900$  and  $1400\text{ cm}^{-1}$  can be attributed to the stretching vibration and bending vibration of  $\text{C}-\text{H}$ , respectively. The strong absorption peak observed at  $1650\text{ cm}^{-1}$  was due to the stretching vibration  $\text{C}=\text{O}$ . In addition, there is no noticeable difference among different samples, which may hint that there are no new functional groups that have characteristic IR absorption peaks. In Figure 2B, the UV curve of GelMA-DOPA has an absorption peak at 280 nm compared to that of GelMA, which may be due to the presence of the catechol groups. To further confirm the presence of the catechol groups, NMR detection was subsequently carried out, as shown in Figure 3.

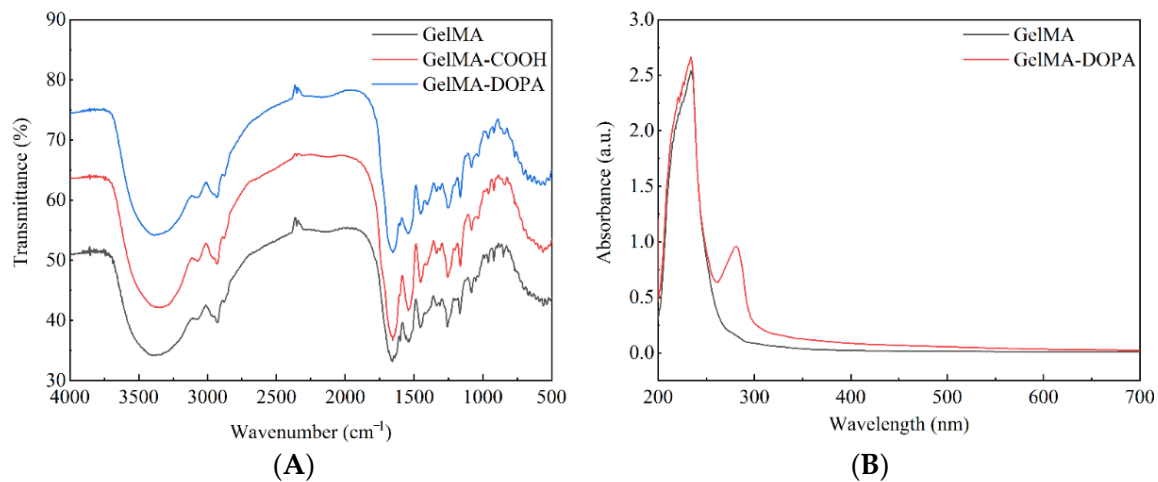


**Figure 2.** IR and UV spectra of different prepolymers. **(A):** IR spectra of GelMA, GelMA-COOH and GelMA-DOPA prepolymers; **(B):** UV spectra of GelMA and GelMA-DOPA prepolymers.

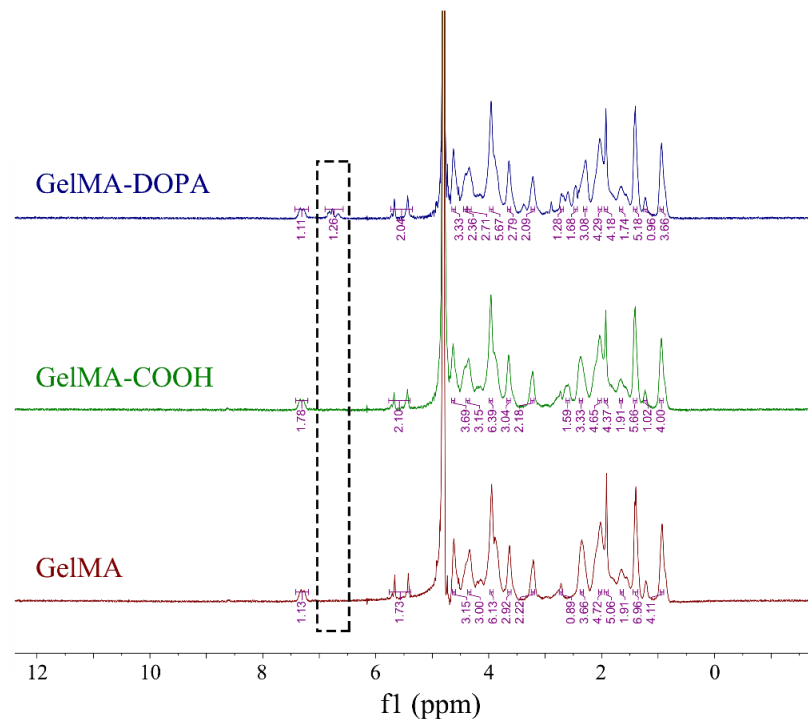


**Figure 3.** NMR hydrogen spectra of GelMA, GelMA-COOH and GelMA-DOPA.

Overall, the hydrogen spectra of GelMA, GelMA-COOH, and GelMA-DOPA were highly similar except for the peak at chemical shift values of 6–7 ppm. Compared with GelMA and GelMA-COOH, GelMA-DOPA shows a unique peak, which is characteristic of the hydrogen atom in the catechol group in dopamine hydrochloride. Therefore, it was proved that the catechol-modified photo-cross-linkable GelMA-DOPA polymer had been successfully synthesized.

In order to determine the contents of catechol groups in the as-synthesized GelMA-DOPA prepolymers, dopamine hydrochloride solutions with different concentrations, i.e., 0.1, 0.2, 0.3, 0.4 and 0.5 mM, were prepared as standard solutions. UV spectra of the solutions were obtained to compare the absorbance value of GelMA-DOPA prepolymers and standard solutions, as shown in Figure 4A. The linearity between concentration and absorbance was established from the measured absorbance values, as shown in Figure 4B.

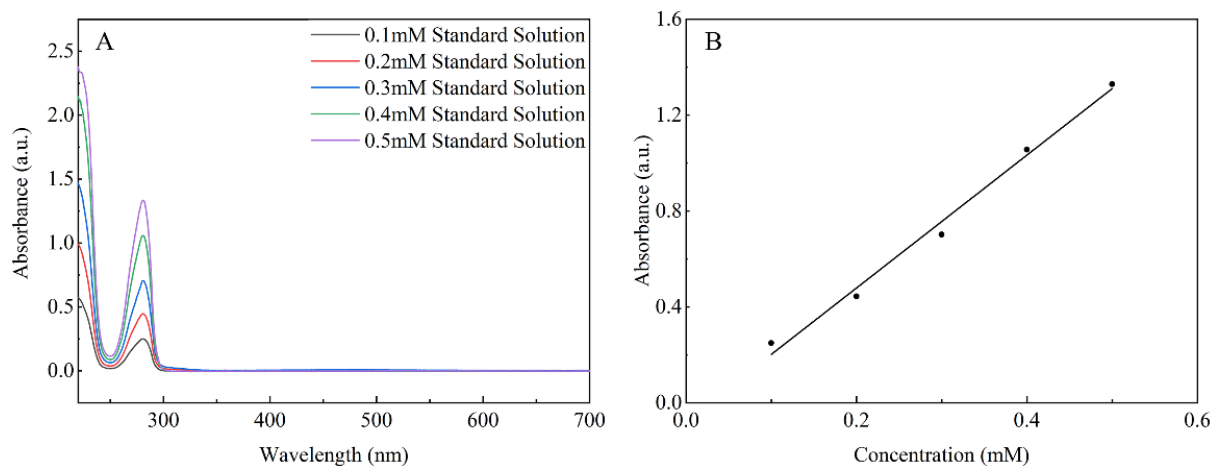


**Figure 4.** (A): UV spectra of the standard solutions of dopamine hydrochloride; (B): the linear relation between the concentration of dopamine hydrochloride and absorbance.

From Figure 4B the function of the fitted straight line is  $y = 2.772x - 0.075$  and  $R^2 = 0.9907$ . Substituting the absorbance value ( $y$ ) of GelMA-DOPA measured in Figure 2B, it can be obtained that  $x = 0.38$ . Accordingly, the concentration of catechol groups in the prepared GelMA-DOPA is 0.38 mM.

### 3.2. Swelling Performances of GelMA and GelMA-DOPA Hydrogels

Hydrogels with 4 different concentrations (5% ( $w/v$ ), 10% ( $w/v$ ), 15% ( $w/v$ ), and 20% ( $w/v$ )) were placed in PBS solution at 37 °C, and all of the hydrogels were able to swell rapidly from 0–1 h, and the swelling equilibrium was reached at 8 h, as shown in Figure 5. Comparing the two types of hydrogels, i.e., GelMA hydrogels and GelMA-DOPA hydrogels, the swelling performances of GelMA-DOPA hydrogels with 10% ( $w/v$ ), 15% ( $w/v$ ), and 20% ( $w/v$ ) concentrations were better than those of GelMA hydrogels with the same concentrations. However, some GelMA-DOPA hydrogels broke up after a prolonged time of immersion. The hydrogels were intact within 12 h of immersion, but started to break. Especially after 24 h of immersion, the GelMA-DOPA hydrogels broke severely with concentrations of 5% ( $w/v$ ) and 10% ( $w/v$ ). In contrast, GelMA-DOPA hydrogels with 20% ( $w/v$ ) were intact in appearance even after 96 h of immersion. Also, the equilibrium swelling rate of 20% ( $w/v$ ) GelMA-DOPA hydrogels was high, reaching  $505.10 \pm 21.30\%$ .

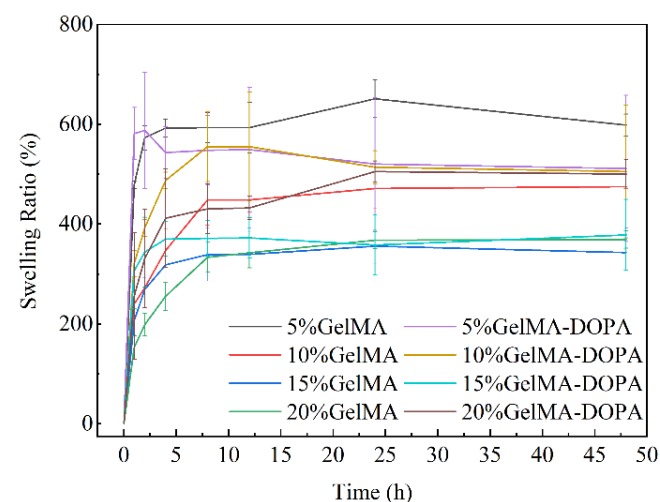


**Figure 5.** The swelling performances of GelMA and GelMA-DOPA hydrogels with different concentrations.

### 3.3. Degradation Performances of GelMA and GelMA-DOPA Hydrogels

As shown in Figure 6, all of the hydrogel samples were placed in a solution of collagenase at 37 °C, and the degradation rates of the GelMA and GelMA-DOPA hydrogels can be controlled by varying the concentration of the hydrogels. The time required for hydrogel degradation increased with the increase of the concentrations. On the 2nd day of the degradation experiment, both two types of hydrogels with a concentration of 5% (*w/v*) degraded completely. On the 3rd day of the experiment, both hydrogels with concentrations of 10% (*w/v*) and 15% (*w/v*) began to degrade noticeably and debris of hydrogel appeared. Only the hydrogel whose concentration was 20% (*w/v*) remained intact in shape. It was found that the degradation rate of GelMA-DOPA hydrogels was higher than that of GelMA hydrogels. All of the GelMA-DOPA hydrogels were completely degraded by 5 days of immersion, while the complete degradation time for 20% (*w/v*) GelMA hydrogels was 10 days. It can be speculated that DOPA is more hydrophilic and can accelerate the degradation process of GelMA-DOPA hydrogels. From this perspective, the degradation behaviors of GelMA-DOPA hydrogels can be modified with further regulation of concentration of DOPA groups.

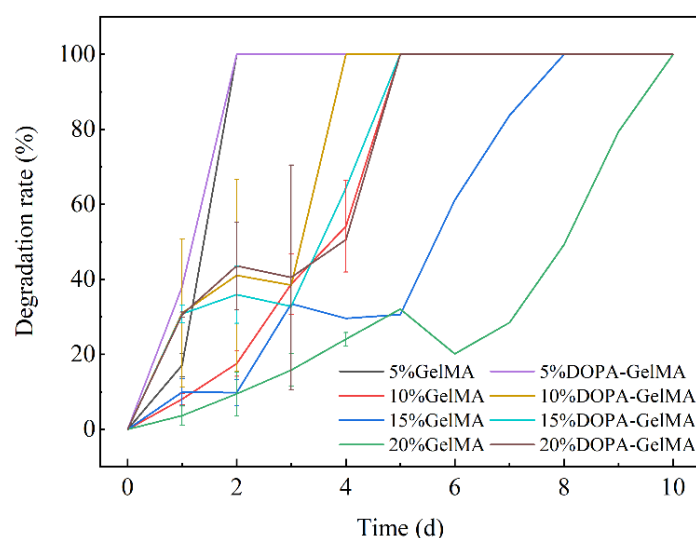


**Figure 6.** Degradation performances of GelMA and GelMA-DOPA hydrogels with different concentrations.

### 3.4. Morphologies of GelMA and GelMA-DOPA Hydrogel Coated Mg Alloys

GelMA and GelMA-DOPA hydrogels with different concentrations, i.e., 5% (*w/v*), 10% (*w/v*), 15% (*w/v*), and 20% (*w/v*), were coated on the surface of Mg alloys, and the morphologies of the surface and cross-sections of samples were observed by SEM. Figure 7A–H show surface morphologies of coatings for the two types of hydrogels, and Figure 7A–D and Figure 7E–H are SEM images of GelMA hydrogel-coated Mg alloys and GelMA-DOPA hydrogel-coated samples, respectively, and Figure 7I shows SEM image of bare Mg alloys pellets. There is no significant difference between the surface morphologies of the two types of hydrogel coatings with different concentrations. Overall, the surface of the hydrogel coating is smooth, and there are few pores or cracks in the coatings. No noticeable difference in cracks was observed between the two types of hydrogel coatings.

SEM images of the cross-section of the two types of hydrogel-coated Mg alloys are shown in Figure 8. Coatings in Figure 8A–D and Figure 8E–H are GelMA hydrogel and GelMA-DOPA hydrogel with different concentrations, respectively. There is no obvious difference in thickness and uniformity between the two types of hydrogel coatings, e.g., the thickness of the coatings is not significantly related to the types and concentrations of the hydrogel. Besides, both of the hydrogel coatings are tightly bonded to the Mg alloys and the thicknesses of all the hydrogel coatings are  $9.62 \pm 1.7 \mu\text{m}$ . Therefore, it is

feasible to prepare GelMA-DOPA hydrogel coatings on the surface of Mg alloys from the perspective of morphologies, and other works on mechanical properties, biocompatibility, and bioactivities of the GelMA-DOPA hydrogel/Mg alloy composites are in progress.

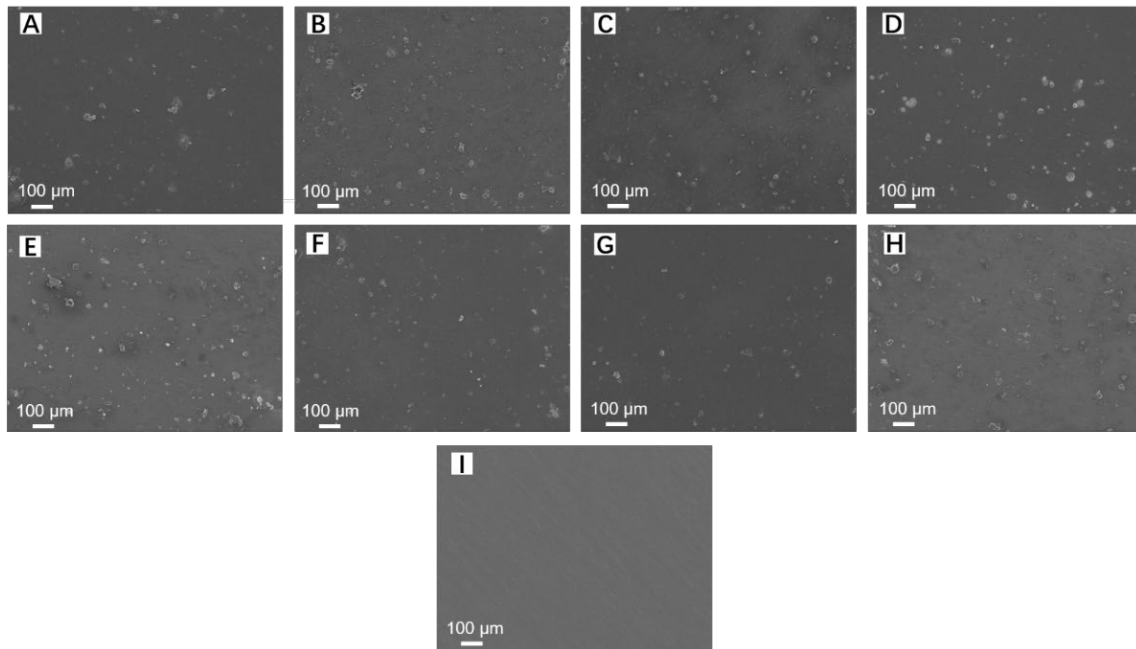


**Figure 7.** SEM images of the surface of GelMA and GelMA-DOPA hydrogel coatings on magnesium alloys, and the coatings of samples are: (A): 5% (*w/v*) GelMA; (B): 10% (*w/v*) GelMA; (C): 15% (*w/v*) GelMA; (D): 20% (*w/v*) GelMA; (E): 5% (*w/v*) GelMA-DOPA; (F): 10% (*w/v*) GelMA-DOPA; (G): 15% (*w/v*) GelMA-DOPA; (H): 20% (*w/v*) GelMA-DOPA; (I): bare WE43 Mg alloy.

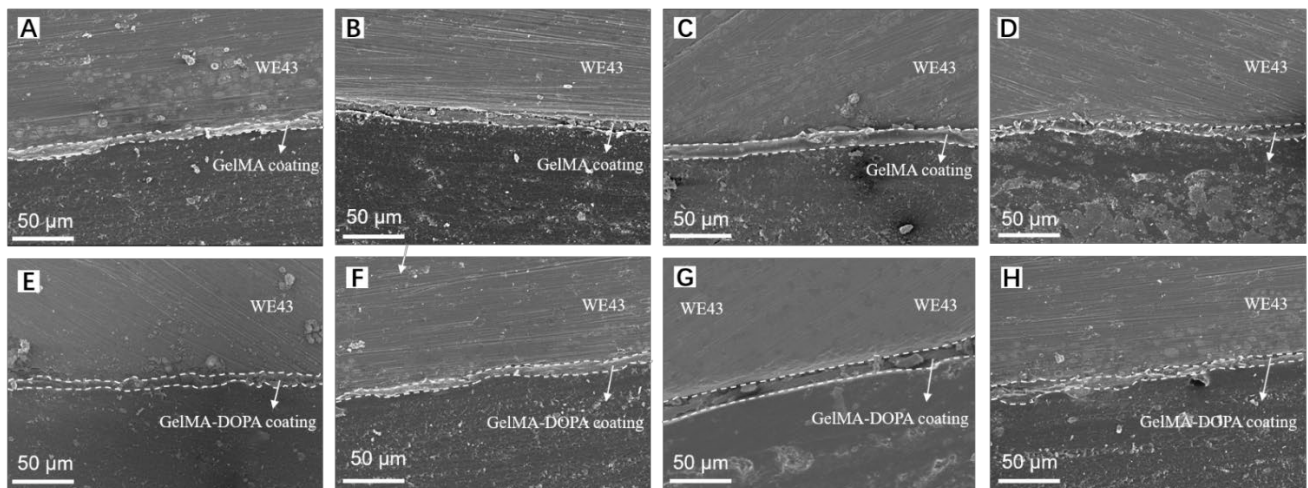


**Figure 8.** SEM images of cross-sections of GelMA and GelMA-DOPA hydrogel coatings on magnesium alloys: (A): 5% (*w/v*) GelMA/Magnesium Alloy; (B): 10% (*w/v*) GelMA/Magnesium Alloy; (C): 15% (*w/v*) GelMA/Magnesium Alloy; (D): 20% (*w/v*) GelMA/Magnesium Alloy; (E): 5% (*w/v*) GelMA-DOPA/Magnesium Alloy; (F): 10% (*w/v*) GelMA-DOPA/Magnesium Alloy; (G): 15% (*w/v*) GelMA-DOPA/Magnesium Alloy; (H): 20% (*w/v*) GelMA-DOPA/Magnesium Alloy.

#### 4. Conclusions

Mussel-inspired modified GelMA hydrogels were prepared and deposited on the surface of WE43 magnesium alloy directly via a dip-coating technique. The chemical groups, swelling properties, and degradation properties of GelMA-DOPA and the morphologies

of the coatings have been investigated. The content of the catechol groups in the GelMA-DOPA hydrogel was deduced to be 0.38 mM based on the calibration method developed. The 5% (*w/v*) hydrogel has the maximum swelling rate, whereas GelMA has a swelling rate of ( $597.99 \pm 22.27\%$ ) and GelMA-DOPA has a swelling rate of ( $511.23 \pm 146.44\%$ ). Overall, hydrogels with a concentration of 20% (*w/v*) of GelMA-DOPA to PBS have better performance in immersion tests. Generally, GelMA-DOPA coatings are smooth and the thickness of coatings is  $9.62 \pm 1.7 \mu\text{m}$  with three times of coating. More systematic experiments are encouraged to be carried out to investigate the mechanical properties and biological performance of the novel GelMA-DOPA/Mg composites.

**Author Contributions:** Conceptualization, X.Z., H.Y. and C.C.; methodology, Y.J. and M.H.; validation, Y.J., M.H. and J.Z.; formal analysis, Y.J., M.H. and T.W.; investigation, C.C. and H.Y.; resources, M.H., Y.J. and H.Y.; data curation, Y.J. and M.H.; writing—original draft preparation, Y.J. and H.Y.; writing—review and editing, J.Z. and X.Z.; supervision, H.Y., X.Z. and C.C.; project administration, M.H. and Y.J.; funding acquisition, H.Y. All authors have read and agreed to the published version of the manuscript.

**Funding:** The work was supported by the project from the Natural Science Foundation of Liaoning Province of China (No. 2020-MS-166), Foundation of the Education Department of Liaoning Province in China (No. QN2019035) and the National Natural Science Foundation of China (No. 81500897).

**Institutional Review Board Statement:** Not applicable.

**Informed Consent Statement:** Not applicable.

**Data Availability Statement:** Not applicable.

**Conflicts of Interest:** The authors declare no conflict of interest.

## References

1. Lin, Z.; Sun, X.; Yang, H. The Role of Antibacterial Metallic Elements in Simultaneously Improving the Corrosion Resistance and Antibacterial Activity of Magnesium Alloys. *Mater. Des.* **2021**, *198*, 109350. [[CrossRef](#)]
2. Li, L.; Cui, L.; Zeng, R.; Li, S.; Chen, X.; Zheng, Y.; Kannan, M. Advances in functionalized polymer coatings on biodegradable magnesium alloys—A review. *Acta Biomater.* **2018**, *79*, 23–36. [[CrossRef](#)]
3. Yu, X.; Huang, W.; Zhao, D.; Yang, K.; Tan, L.; Zhang, X.; Li, J.; Zhang, M.; Zhang, S.; Liu, T.; et al. Study of engineered low-modulus Mg/PLLA composites as potential orthopaedic implants: An in vitro and in vivo study. *Colloids Surf. B-Biointerfaces* **2019**, *174*, 280–290. [[CrossRef](#)]
4. Liu, C.; Yang, H.; Wan, P.; Wang, K.; Tan, L.; Yang, K. Study on biodegradation of the second phase Mg<sub>17</sub>Al<sub>12</sub> in Mg-Al-Zn Alloys: In vitro experiment and thermodynamic calculation. *Mater. Sci. Eng. C-Mater. Biol. Appl.* **2014**, *35*, 1–7. [[CrossRef](#)]
5. Ji, Y.; Yu, X.; Zhu, H. Fabrication of Mg Coating on PEEK and Antibacterial Evaluation for Bone Application. *Coatings* **2021**, *11*, 1010. [[CrossRef](#)]
6. Wu, W.; Wang, Z.; Zang, S.; Yu, X.; Yang, H.; Chang, S. Research Progress on Surface Treatments of Biodegradable Mg Alloys: A Review. *Acs Omega* **2020**, *5*, 941–947. [[CrossRef](#)]
7. Wieja, F.; Jacobs, G.; Stein, S.; Kopp, A.; van Gaalen, K.; Kroger, N.; Zinser, M. Development and validation of a parametric human mandible model to determine internal stresses for the future design optimization of maxillofacial implants. *J. Mech. Behav. Biomed. Mater.* **2022**, *125*, 104893. [[CrossRef](#)]
8. Bommala, V.; Krishna, M.; Rao, C. Magnesium matrix composites for biomedical applications. *J. Magnes. Alloys* **2019**, *7*, 72–79. [[CrossRef](#)]
9. Wu, W.; Yu, X.; Zhao, Y.; Jiang, X.; Yang, H. Characterization and Biocompatibility of Insoluble Corrosion Products of AZ91 Mg Alloys. *Acs Omega* **2019**, *4*, 15139–15148. [[CrossRef](#)]
10. Hu, Y.; Bi, Y.; He, D.; Yu, H.; Li, Y. Research Progress on Surface Modification of Biodegradable Magnesium and Magnesium Alloys. *Surf. Technol.* **2019**, *48*, 11–19.
11. Rahim, S.; Joseph, M.; Sampath Kumar, T.; Hanas, H. Recent Progress in Surface Modification of Mg Alloys for Biodegradable Orthopedic Applications. *Front. Mater.* **2022**, *9*, 848980. [[CrossRef](#)]
12. Narayanan, T.; Park, I.; Lee, M. Strategies to improve the corrosion resistance of microarc oxidation (MAO) coated magnesium alloys for degradable implants: Prospects and challenges. *Prog. Mater. Sci.* **2014**, *60*, 1–71. [[CrossRef](#)]
13. Li, C.; Feng, X.; Fan, X.; Yu, X.; Yin, Z.; Konnan, M.; Chen, X.; Guan, S.; Zhang, J.; Zeng, R. Corrosion and Wear Resistance of Micro-Arc Oxidation Composite Coatings on Magnesium Alloy AZ31-The Influence of Inclusions of Carbon Spheres. *Adv. Eng. Mater.* **2019**, *21*, 1900446. [[CrossRef](#)]

14. Wan, Y.; Wang, Y.; Wang, Q.; Tan, L.; Yang, K.; Li, Y.; Li, W. Study on Biodegradable Property of Surface Modified AZ31B Magnesium Alloy in Different Simulated Body Fluid. *Mater. Rev.* **2011**, *25*, 66–69, 86.
15. Liu, G.; Hu, J.; Ding, Z.; Wang, C. Bioactive calcium phosphate coating formed on micro-arc oxidized magnesium by chemical deposition. *Appl. Surf. Sci.* **2011**, *257*, 2051–2057. [[CrossRef](#)]
16. Zhang, D.; Peng, F.; Liu, X. Protection of magnesium alloys: From physical barrier coating to smart self-healing coating. *J. Alloys Compd.* **2021**, *853*, 157010. [[CrossRef](#)]
17. Fan, X.; Huo, Y.; Li, C.; Kannan, M.; Chen, X.; Guan, S.; Zeng, R.; Ma, Q. Corrosion resistance of nanostructured magnesium hydroxide coating on magnesium alloy AZ31: Influence of EDTA. *Rare Met.* **2019**, *38*, 520–531. [[CrossRef](#)]
18. Guo, L.; Gu, C.; Feng, J.; Guo, Y.; Jin, Y.; Tu, J. Hydrophobic epoxy resin coating with ionic liquid conversion pretreatment on magnesium alloy for promoting corrosion resistance. *J. Mater. Sci. Technol.* **2020**, *37*, 9–18. [[CrossRef](#)]
19. Lin, Z.; Wang, T.; Yu, X.; Sun, X.; Yang, H. Functionalization treatment of micro-arc oxidation coatings on magnesium alloys: A review. *J. Alloys Compd.* **2021**, *879*, 160453. [[CrossRef](#)]
20. Liu, W.; Li, T.; Yang, C.; Wang, D.; He, G.; Cheng, M.; Wang, Q.; Zhang, X. Lithium-Incorporated Nanoporous Coating Formed by Micro Arc Oxidation (MAO) on Magnesium Alloy with Improved Corrosion Resistance, Angiogenesis and Osseointegration. *J. Biomed. Nanotechnol.* **2019**, *15*, 1172–1184. [[CrossRef](#)]
21. Lin, X.; Tan, L.; Zhang, Q.; Yang, K.; Hu, Z.; Qiu, J.; Cai, Y. The in vitro degradation process and biocompatibility of a ZK60 magnesium alloy with a forsterite-containing micro-arc oxidation coating. *Acta Biomater.* **2013**, *9*, 8631–8642. [[CrossRef](#)]
22. Elmensouri, G.; Kara, I.; Ahlatci, H.; Turen, Y. Wear Resistance of Sheet Magnesium Alloy AZ31 with Micro Arc Oxidation Coatings after Shot Peening. *Met. Sci. Heat Treat.* **2021**, *63*, 426–429. [[CrossRef](#)]
23. Fischerauer, S.; Kraus, T.; Wu, X.; Tangl, S.; Sorantin, E.; Hanzi, A.; Löffler, J.; Uggowitzer, P.; Weinberg, A. In vivo degradation performance of micro-arc-oxidized magnesium implants: A micro-CT study in rats. *Acta Biomater.* **2013**, *9*, 5411–5420. [[CrossRef](#)]
24. Wu, Y.; Wang, Y.; Tian, S.; Li, H.; Zhao, Y.; Jia, D.; Zhou, Y. Formation mechanism, degradation behavior, and cytocompatibility of a double-layered structural MAO/rGO-CaP coating on AZ31 Mg. *Colloids Surf. B-Biointerfaces* **2020**, *190*, 110901. [[CrossRef](#)]
25. Li, C.; Yu, C.; Zeng, R.; Zhang, B.; Cui, L.; Wan, J.; Xia, Y. In vitro corrosion resistance of a Ta<sub>2</sub>O<sub>5</sub> nanofilm on MAO coated magnesium alloy AZ31 by atomic layer deposition. *Bioact. Mater.* **2020**, *5*, 34–43. [[CrossRef](#)]
26. Shang, W.; Wu, F.; Wang, Y.; Baboukani, A.; Wen, Y.; Jiang, J. Corrosion Resistance of Micro-Arc Oxidation/Graphene Oxide Composite Coatings on Magnesium Alloys. *Acs Omega* **2020**, *5*, 7262–7270. [[CrossRef](#)]
27. Shang, W.; Chen, B.; Shi, X.; Chen, Y.; Xiao, X. Electrochemical corrosion behavior of composite MAO/sol-gel coatings on magnesium alloy AZ91D using combined micro-arc oxidation and sol-gel technique. *J. Alloys Compd.* **2009**, *474*, 541–545. [[CrossRef](#)]
28. Liao, S.; Chang, C.; Chen, C.; Lee, C.; Lin, W. Functionalization of pure titanium MAO coatings by surface modifications for biomedical applications. *Surf. Coat. Technol.* **2020**, *394*, 125812. [[CrossRef](#)]
29. Liu, T.; Weng, W.; Zhang, Y.; Sun, X.; Yang, H. Applications of Gelatin Methacryloyl (GelMA) Hydrogels in Microfluidic Technique-Assisted Tissue Engineering. *Molecules* **2020**, *25*, 5305. [[CrossRef](#)]
30. Sun, M.; Sun, X.; Wang, Z.; Guo, S.; Yu, G.; Yang, H. Synthesis and Properties of Gelatin Methacryloyl (GelMA) Hydrogels and Their Recent Applications in Load-Bearing Tissue. *Polymers* **2018**, *10*, 1290. [[CrossRef](#)] [[PubMed](#)]
31. Liu, T.; Jin, M.; Zhang, Y.; Weng, W.; Wang, T.; Yang, H.; Zhou, L. K<sup>+</sup>/Sr<sup>2+</sup>/Na<sup>+</sup> triple-doped hydroxyapatites/GelMA composite hydrogel scaffold for the repair of bone defects. *Ceram. Int.* **2021**, *47*, 30929–30937. [[CrossRef](#)]
32. Weng, W.; Wu, W.; Yu, X.; Sun, M.; Lin, Z.; Ibrahim, M.; Yang, H. Effect of GelMA Hydrogel Coatings on Corrosion Resistance and Biocompatibility of MAO-Coated Mg Alloys. *Materials* **2020**, *13*, 3834. [[CrossRef](#)] [[PubMed](#)]
33. Cheng, H.; Yue, K.; Kazemzadeh-Narbat, M.; Liu, Y.; Khalilpour, A.; Li, B.; Zhang, Y.; Annabi, N.; Khademhosseini, A. Mussel-Inspired Multifunctional Hydrogel Coating for Prevention of Infections and Enhanced Osteogenesis. *Acs Appl. Mater. Interfaces* **2017**, *9*, 11428–11439. [[CrossRef](#)] [[PubMed](#)]
34. Liu, T.; Zhang, Y.; Sun, M.; Jin, M.; Xia, W.; Yang, H.; Wang, T. Effect of Freezing Process on the Microstructure of Gelatin Methacryloyl Hydrogels. *Front. Bioeng. Biotechnol.* **2021**, *9*, 810155. [[CrossRef](#)] [[PubMed](#)]